MEASUREMENTS ON SIGMA-PHI CHV+ SKEWQUAD CORRECTOR PROTOTYPE FOR THE DAΦNE MAIN RINGS

*B. Bolli, N. Ganlin, F. Iungo, M. Paris, M. Preger, C. Sanelli,
F. Sardone, F. Sgamma, M. Troiani*

1. Introduction

The first prototype of a combined function corrector, consisting in a square iron frame with two separately powered dipole windings (CH and CV) and a skew-quadrupole coil (SQ), in the following called the HVSQ Corrector, built by Sigma-Phi ( ) , Vannes Cedex (France), was delivered to LNF on March 1, 1996, together with other two prototypes, the Square HV (Horizontal/Vertical) Corrector Magnet [1] and the Rectangular HV Corrector Magnet [2]. The first two magnets will be installed in the Main Rings in the regions where the vacuum chamber has a circular shape, the third will be used in the achromats, where the chamber has a larger size in the horizontal direction.

These Corrector Magnets were designed by LNF staff and Fig. 1 shows a picture of HVSQ. Table I gives its main parameters.
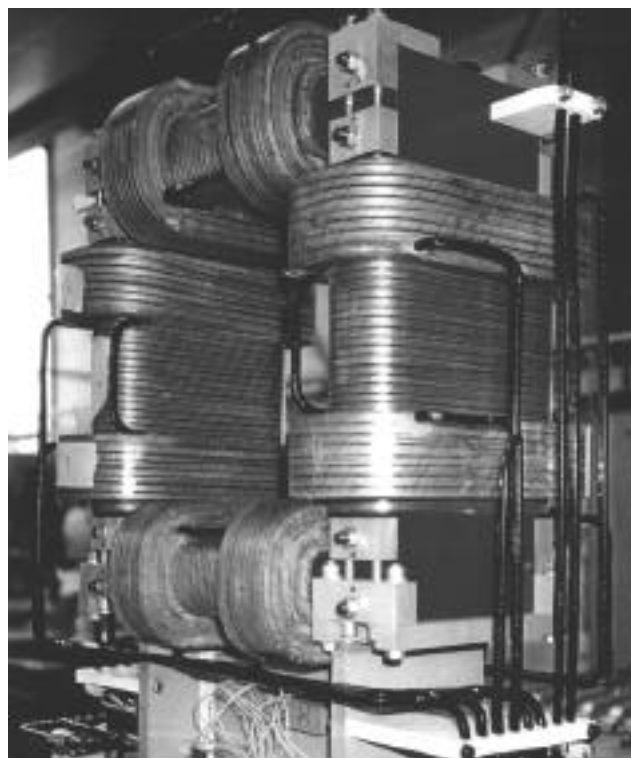
Fig. 1 - Pictorial view of the HVSQ Corrector Magnet

Table I - HVSQ Corrector Magnet prototype parameters.

Rectangular Corrector H/V	units	CH	CV	SQ
Energy	MeV	510	510	510
Magnet Gap	mm	300	300	300
Nominal Field	Gauss	267	267	-
Nominal Gradient	Gauss/cm	-	-	83
Magnetic Length (Design)	m	0.45	0.45	0.26
Number of turns per pole		36	36	31
Nominal Current	A	191	191	235
Copper Conductor	mm∗mm	6∗6	6∗6	6∗6
Cooling Hole Diameter	mm	3.5	3.5	3.5

2. Electrical measurements

The resistance of the HVSQ Corrector Magnet was measured by means of a micro-ohm-meter (AOIP mod. OM 20) at room temperature.

The measured values were:

Horizontal	0.0266	@	23 °C
Vertical	0.0265	@	23 °C
Skew Quad	0.1037	@	23 °C

The same measurement were accomplished by using the Volt-Ampere method and the following data were measured:

Horizontal   5.05 V @ 191A, corresponding to 26 m
Vertical   5.05 V @ 191 A, corresponding to 26 m
Skew Quad   24.75 V @ 235 A, corresponding to 105 m

These values were obtained at the same room temperature as in the preceding measurement. The agreement between the results obtained with the two different methods is very good.

The inductance and resistance of the three magnet prototypes were also measured by means of a LCR meter (LCR meter HP 4284 A) at different frequencies. The results are shown in Figure 2. The corresponding dc values can be extrapolated from these data. They are consistent with the measured and design data.
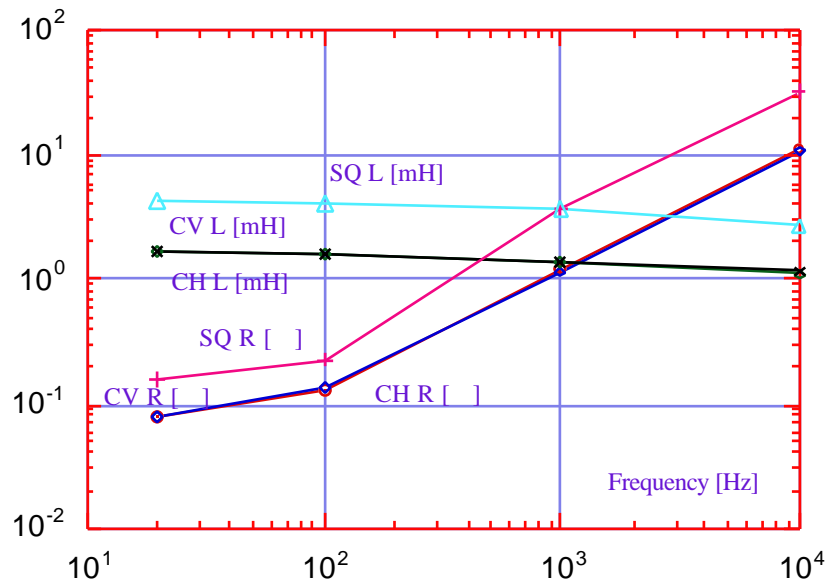
Fig. 2 *- Resistance and inductance versus frequency for the Square Corrector Magnet*

Thermal measurements were also accomplished and the worst figures for the HVSQ Corrector Magnet is listed in Table II (horizontal and vertical dipole corrector coils) and Table III (skew quadrupole corrector coil).

**Table II** - Temperature rise of dipole corrector coils

Time (min)	0	15	30	45
Temperature (°C)	24	27.3	27.6	27.6

Table III - Temperature rise of skew quadrupole corrector coil

Time (min)	0	15	30	45	60	75
Temperature (°C)	23	31	31	32.2	32.5	33.0

3. Magnetic measurements on the horizontal/vertical dipole corrector

The horizontal and vertical components of the field at the magnet center have been separately measured as a function of the current in the corresponding coil (in the following we indicate with CH the horizontal corrector coil, which generates the vertical field component, and with CV the other one). The difference between the two measurement is negligible, and therefore we show the common behaviour in Fig. 3: it is linear over the operating range. Since the magnet was powered by a unipolar power supply, it was not possible to check carefully the behaviour of remanent field when inverting the corrector polarity, which, of course, will be done in the normal operation of the ring with the final bipolar power supplies. However, the remanent fields observed during the cycling operation with the available equipment are less than 2 G.
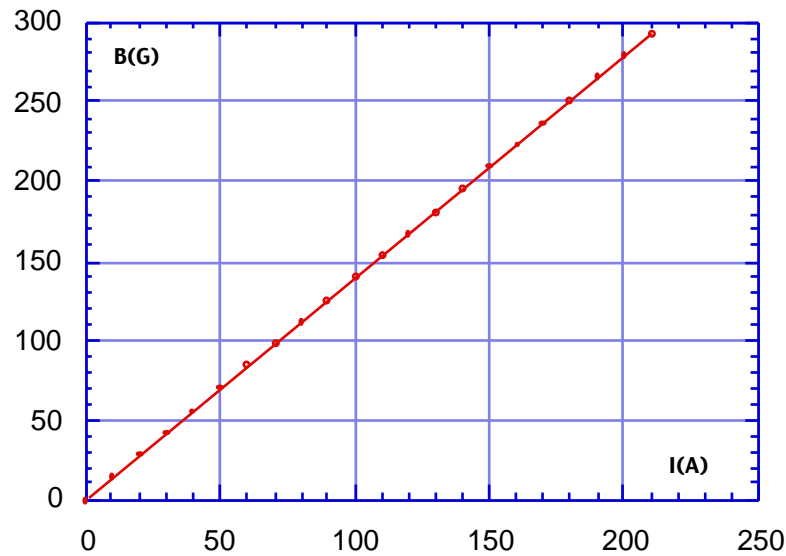
Fig. 3 *- Field components at magnet center versus current.*

We have also measured the dependence of each component on the current, at the magnet center, in the corresponding coil with the <u>other</u> coil set at the maximum current. Taking into account the remanent field coming from the cycling procedure with both coils excited, the difference with respect to the previous measurement with the other coil switched off is less then 0.2% on the whole operating range.

However, the above mentioned check is not enough to demonstrate the independence of the corrections in the two planes. We have therefore measured the vertical component of the field on a vertical plane perpendicular to the magnet axis at its midpoint inside the good field region up to distance of 30 mm from the longitudinal axis in both the horizontal and vertical directions with CH set at the nominal current. The result is shown on an expanded scale in Fig. 4 as a function of the horizontal position, each curve corresponding to a different vertical position. The field is constant within   2% in the good field region (± 30 mm in both directions).
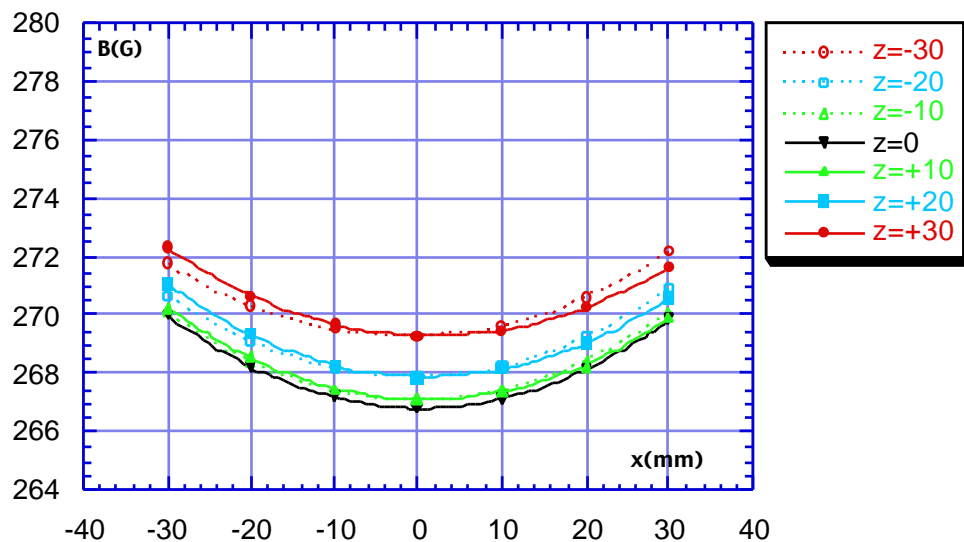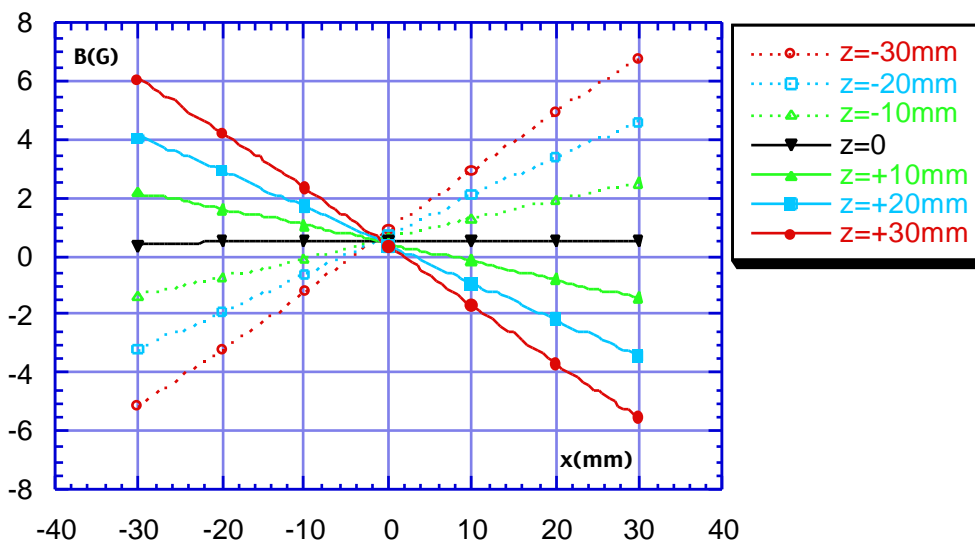

Fig. 4 *- Vertical field component at magnet center with CH @ 191 A and CV off*
(expanded scale)

The situation changes significantly when both corrector coils are switched on: Figure 5 shows the vertical field component, on the same scale as in Fig.4, when both corrector coils are set at the nominal current. The variation of the field inside the good field region increases to 5% and depends both on the horizontal and vertical positions. It is clear that this implies that the orbit corrections in the two planes are influenced by each other.
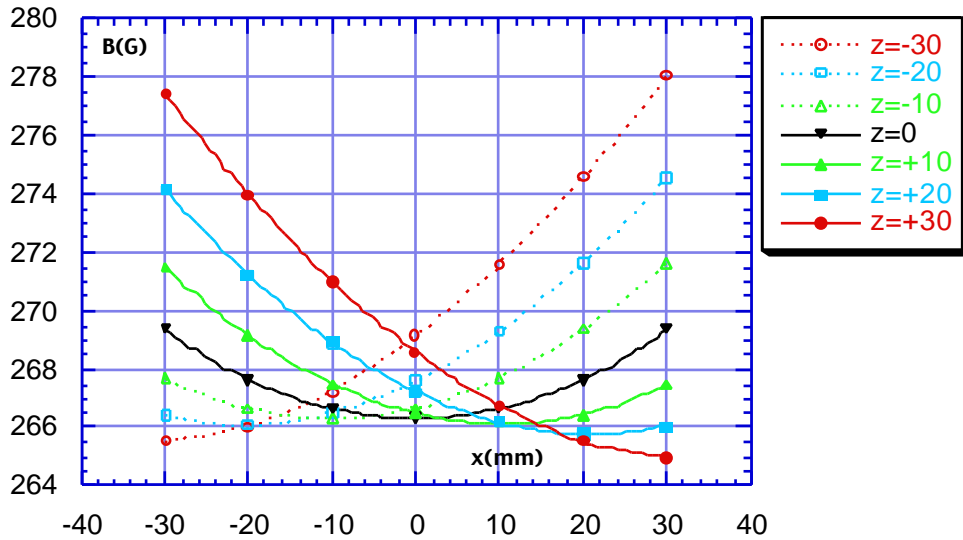
Fig. 5 *- Vertical field component at magnet center with CH and CV @ 191 A*
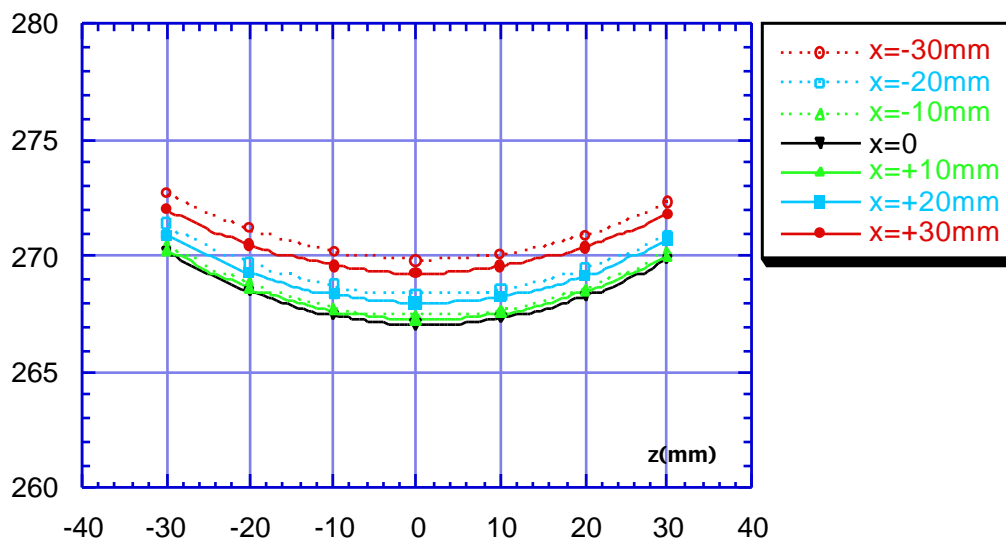*(expanded scale)*

We have therefore measured the vertical field component when only <u>the other</u> corrector (CV) is set to the nominal current (CH off), and the result is shown in Fig. 6. The behaviour is almost linear in both directions and the center appears to be displaced horizontally by -2 mm.
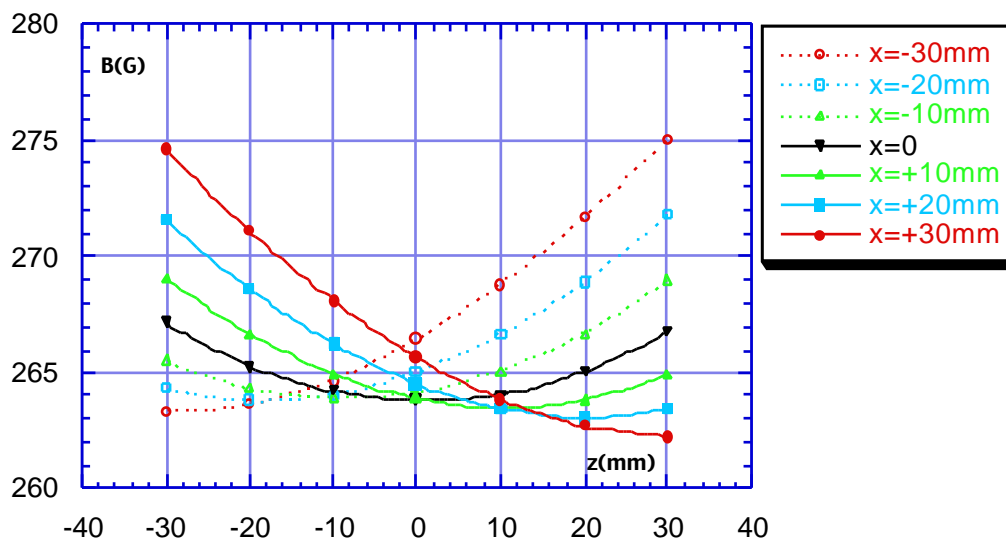

Fig. 6 *- Vertical field component at magnet center with CV @ 191 A (CH off)*

We have then compared the field measured with both coils excited with the sum of the fields measured with each coil excited separately, namely the field given in Fig. 5 with the sum of those given in Fig. 4 and Fig. 6. The difference between the corresponding points is 1.10 G for x = z = 0 and within 1.15 G and 0.95 G in all the other points. We have therefore an offset, coming from the different cycling procedures in the three separate measurements, but, apart from this effect, the fields created by the two coils add linearly in the good field region.

For sake of completeness, we show in Figs. 7÷9 the corresponding measurements for the horizontal field component. In this case the above mentioned difference is 1.65 G at the magnet center and within 1.10 G and 2.30 G in the other points. Since we are now considering the correction in the vertical plane, the field is shown on an expanded scale versus the vertical coordinate (z), with the horizontal one (x) as a parameter.

Fig. 7 - *Horizontal field component at magnet center with CV @ 191 A and CH off (expanded scale)*
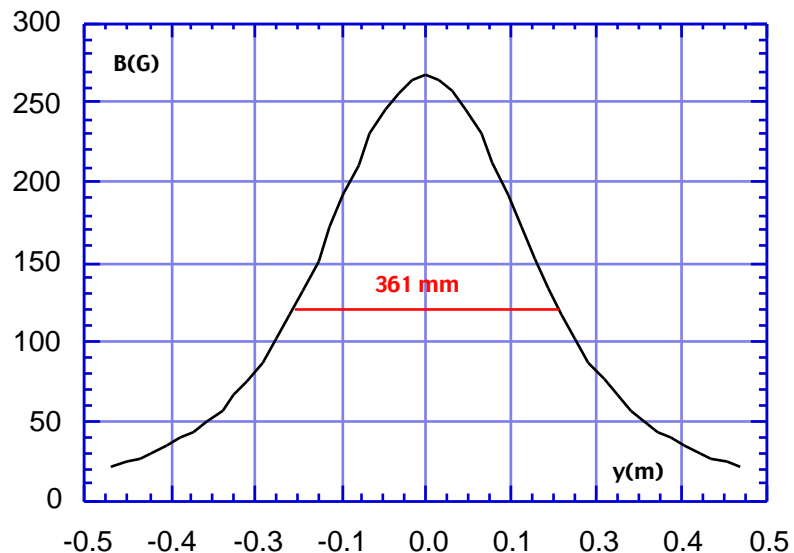

Fig. 8 - *Horizontal field component at magnet center with CV and CH @ 191 A (expanded scale)*
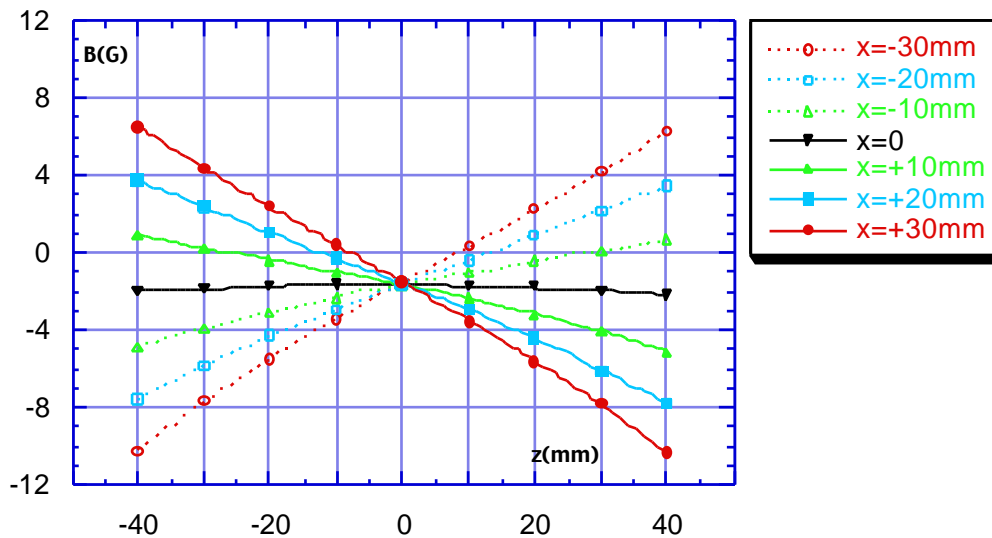
Fig. 9 - Horizontal field component at magnet center with CH @ 191 A (CV off)

The behaviour of the field along the longitudinal (y) direction (parallel to the magnet axis) has been measured in steps of 20 mm along straight lines parallel to the magnet axis at different horizontal and vertical distances from it in steps of 10 mm inside the good field region. The field on the central axis is shown in Fig. 10 for the vertical component, the horizontal one being the same within a fraction of G. The full width at half maximum is 361 mm, but there are long tails, not negligible even at half a meter from the magnet center. This should be kept in mind for those correctors located into the ring near other magnetic elements, since the calibration could change significantly due to the absorption of the field lines by the yokes of the neighbouring magnets.

Fig. 10 - Horizontal field component along the magnet axis with CV @ 191 A

The value of the field integral taken along lines parallel to the magnet axis at different horizontal and vertical positions are given in Fig. 11 and Fig. 12 for the vertical and horizontal component respectively (the scale is expanded).
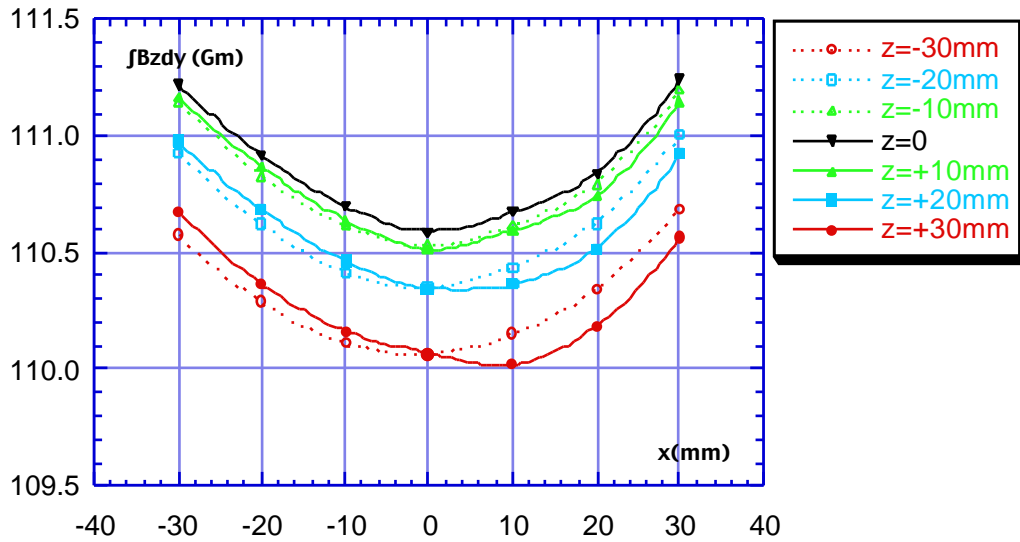
Fig. 11 - *Integrated vertical component with CH @ 191 A and CV off (expanded scale)*
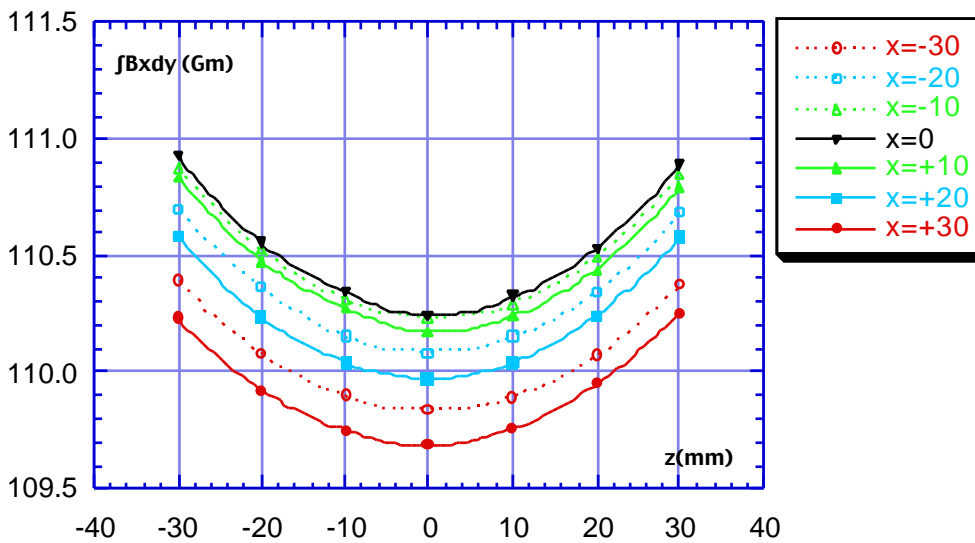

Fig. 12 - *Integrated horizontal component with CV @ 191 A and CH off (expanded scale)*

From the comparison of the last two figures we point out that there is a difference of 0.3% in the calibration between the horizontal and vertical components. The calibration changes by ±0.6% within the good field region with respect to its value taken at the magnet center. Left-right and up-down asymmetries are negligible.

Taking for the calibration the average between the two components, we get for the angular kick to the beam:

$$(mrad) = 1.73 \times 10^{-2} \, I \, (A) / E \, (GeV)$$

By fitting the curves in Fig. 11 and Fig. 12 with a polynomial, we find a small integrated sextupole term. Averaging between the two correctors:

$$S\ (T/m) = \ (\ \partial^2 B_{z,x}/\ \partial x, z^2)\ dy = 6.8 \times 10^{-4}\ I\ (A)$$

Due to the close proximity of the two rings and the peculiar design of the corrector magnet, stray field on the outer side of the coils can reach non negligible values. For this reason, we have measured the vertical field component on the horizontal symmetry plane along a straight line perpendicular to the magnet axis at its center with the horizontal coil CH at the nominal current. The result is shown in Fig. 13, where the origin of the horizontal coordinate is at the magnet center, like in all the previous plots, and both coils are excited at the maximum current. The difference between the fields measured on the right and left sides of the magnet is negligible and the field does not change significantly when also CV is switched on. On the same plot we show also the horizontal component measured at the same points with CV at the nominal current, and also in this case the field value is the same on the right and left sides of the magnet and does not change when CH is switched on. Both components have the same direction on the two sides of the corrector.
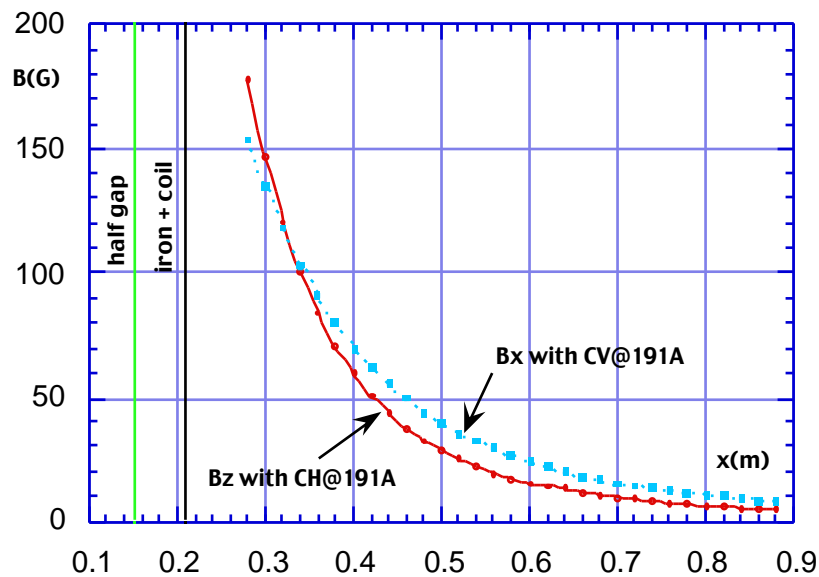
Fig. 13 - Field components of the stray field on the horizontal symmetry plane

4. Magnetic measurements on the skew quadrupole corrector

The dependence of the gradient on the excitation current has been measured by taking the difference between the field values at 30 mm on the left and right sides with respect to the magnet axis for the horizontal component, and between up and down at the same distance for the vertical one. The result is the same, within 0.6%, for the two components, and is shown in Fig. 14: there is no observable deviation from linearity.
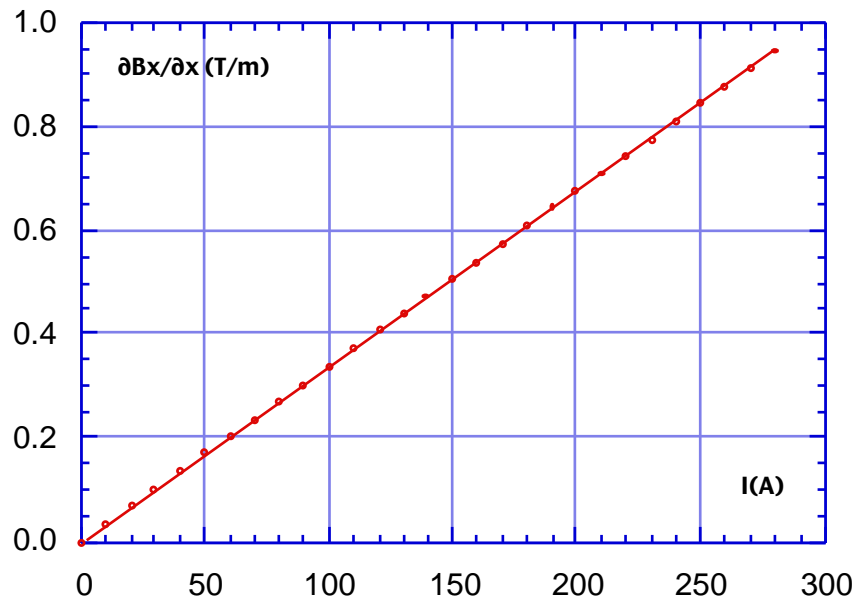
Fig. 14 - Gradient at magnet center versus excitation current

In order to check the independence of the three correction functions (horizontal dipole, vertical dipole and skew quadrupole) we have measured the field inside the good field region on a plane perpendicular to the magnet axis passing through the magnet center, a first time with only the skew quadrupole coil SQ at the nominal current (235 A) and a second one with all the three coils switched on (191 A in CH and CV). We have then compared the measured values in the latter configuration with the sum of those obtained with the three coils excited separately, following the same procedure described in Section 3 for CH and CV. For the horizontal component we find an offset of 1.9% with respect to the center field, plus a maximum deviation of ±0.6% at the boundary of the good field region. For the vertical component these values are 1.5% and ±0.5% respectively.

We have then measured both field components in steps of 20 mm along straight lines parallel to the magnet axis at different horizontal and vertical distances from it in steps of 10 mm inside the good field region. The field on the central axis is shown in Fig. 15 for the vertical component, the horizontal one being the same within a fraction of G. The full width at half maximum is 256 mm, but there are long tails, not negligible even at half a meter from the magnet center. This should be kept in mind for those correctors located into the ring near other magnetic elements, since the calibration could change significantly due to the absorption of the field lines by the yokes of the neighbouring magnets. The integrated gradient calculated from the field integrals at ±30 mm from the magnet axis is:

$$\int (\partial Bx/\partial x)dy \ (T) = \int (\partial Bz/\partial z)dy \ (T) = 9.52 \times 10^{-4} \ I(A)$$
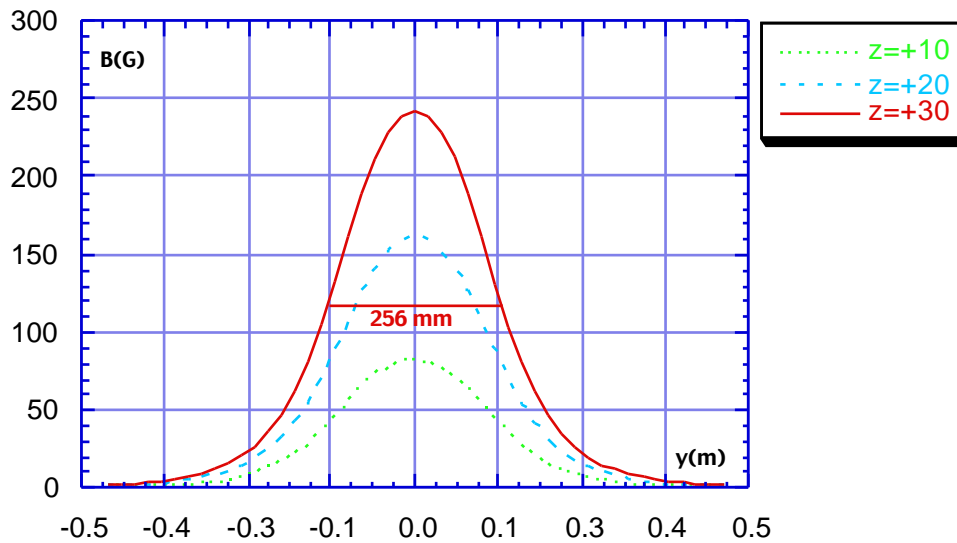
Fig. 15 *- Vertical field component at different heights with respect to the magnet axis with SQ @ 235 A, CH and CV off*

The stray field outside the magnet has been measured along a straight line on the horizontal plane perpendicular to the magnet axis with SQ at the nominal current. In this case the field has opposite directions on the two sides of the yoke. In order to give a complete description of the effects of the different coils we show in Fig. 16 the vertical component of the stray field on both sides of the magnet with CH, CV and SQ set separately at their nominal currents. Figure 17 gives the horizontal component. The straight lines indicate the position of the magnet gap: the measured values start somewhat far from these lines, due to the place taken by the yoke, the excitation coils and the Hall probe support.
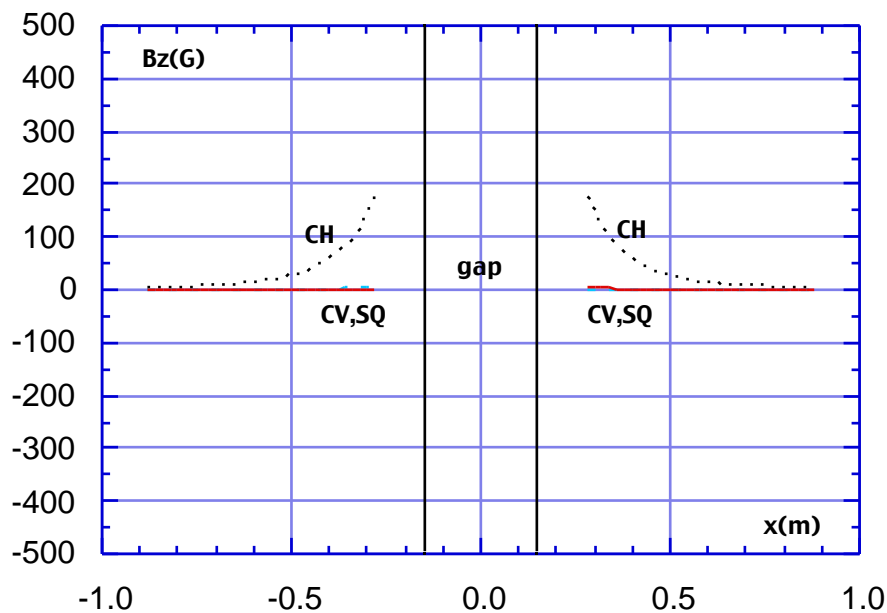
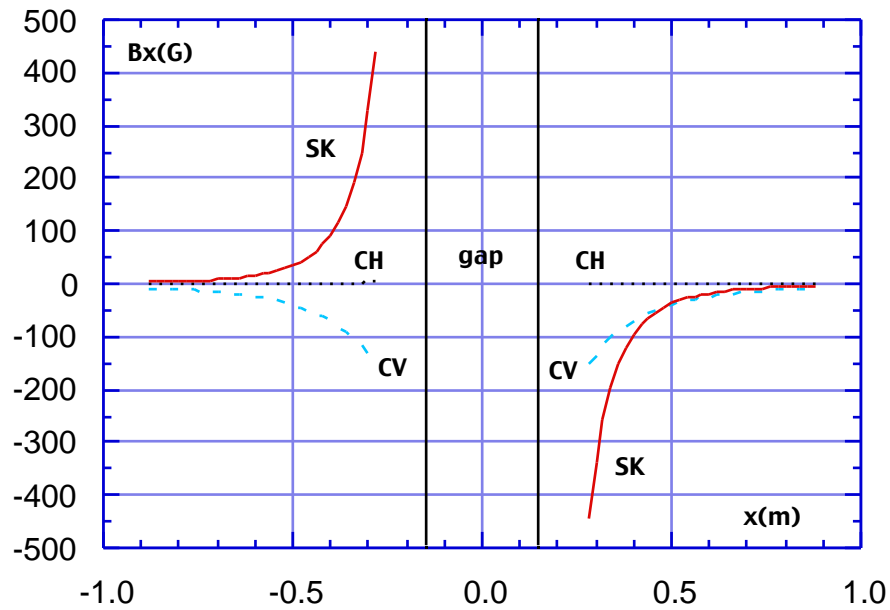***Fig.16*** *- Vertical component of the stray field on the horizontal plane outside the magnet*

Fig. 17 - *Horizontal component of the stray field on the horizontal plane outside the magnet*

The magnet has been finally analysed with the rotating coil system [3], in order to test its field quality and determine the high order component distribution. The output of the system, at the nominal excitation current in SQ (CH and CV off), is shown in Fig. 18, together with the most important contributions to the deviation from the ideal quadrupole component on a circle of 30 mm radius around the magnet axis. A sextupole component of 0.1% is the dominant high order term. Fig. 19 shows the behaviour of the integrated gradient, of the sextupole and octupole contributions to the field deviation as a function of the excitation current. The integrated gradient is linear and the high order contributions are fairly constant over the whole operating range.
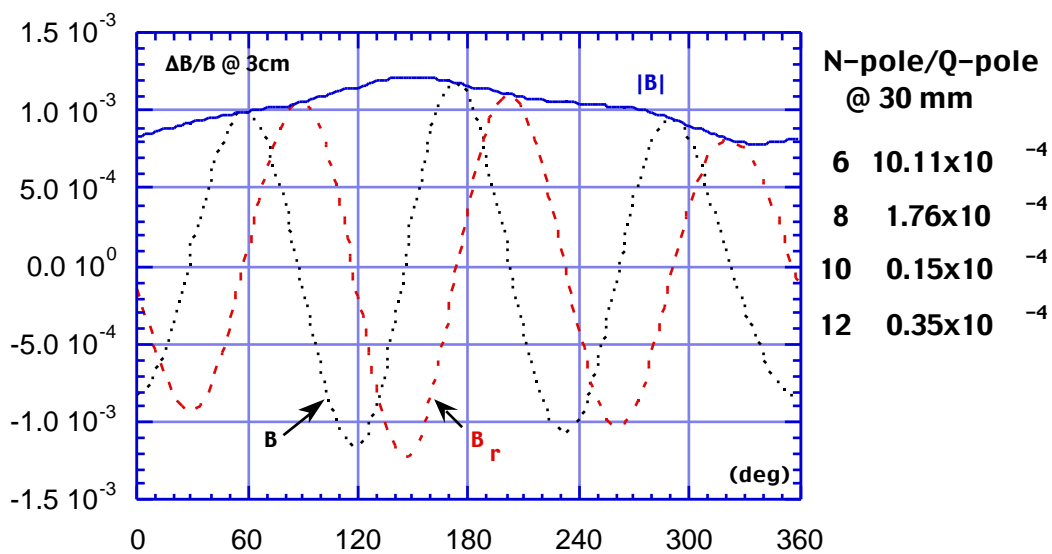

Fig. 18 - *Deviation from the ideal quadrupole field on a circle of 30 mm diameter around the magnet axis (SQ @ 235 A).*
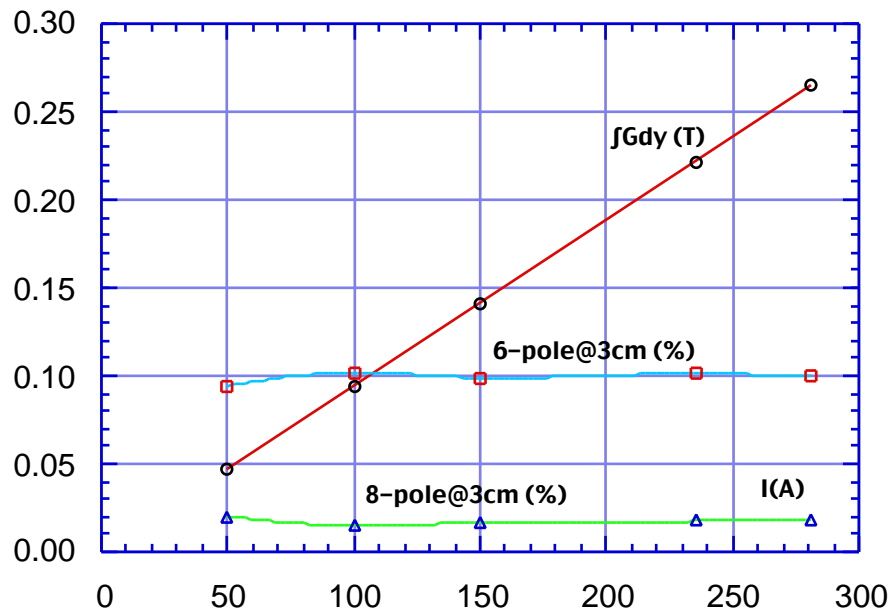
Fig. 19 *- Integrated gradient, sextupole and octupole contributions to the field error @ 3 cm as a function of excitation current.*

As a last check we measured the field quality with SQ, CH and CV at the nominal current, with SQ and CH and with SQ and CV. In these three measurements the dominant contribution comes from the sextupole term of the dipole correctors, which is clearly visible in the figures of Section 3. Figure 20 shows the output with SQ and CH at the nominal current. It should be noted that the scale is a factor of ten larger than in Fig. 18. The integrated sextupole term calculated from the output of the rotating coil system is 0.16 T/m. Taking into account that the contribution coming from the sextupole coil is exactly in phase with that coming from the dipole one, this value agrees within 10% with that obtained in Section 3 by fitting the field integral at different distances from the magnet axis.
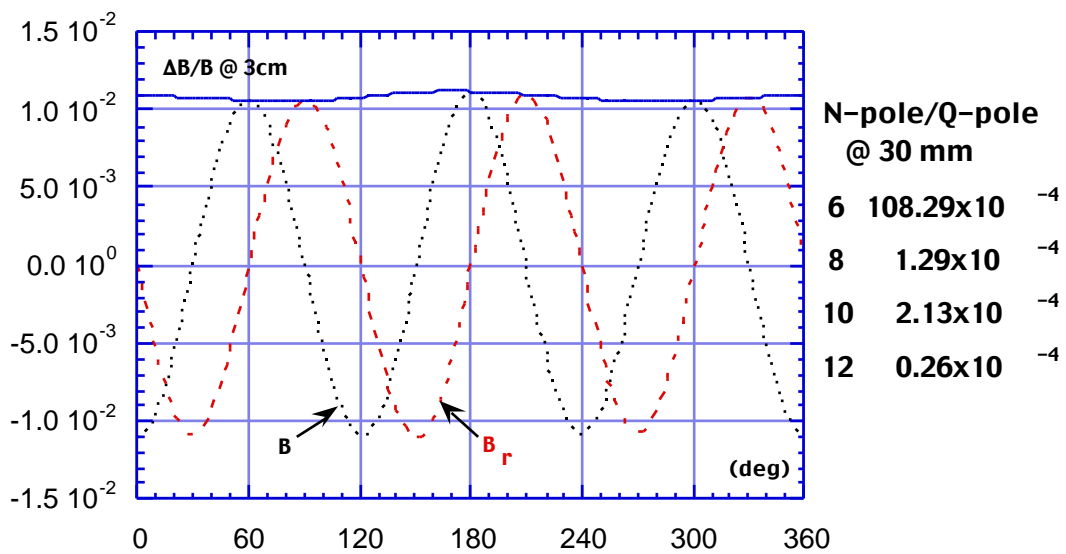

Fig. 20 *- Deviation from the ideal quadrupole field on a circle of 30 mm diameter around the magnet axis (SQ @ 235 A, CH @ 191 A).*

5. Conclusions

The HVSQ Corrector Magnet prototype has been fully characterised at LNF. The measurement confirmed the reliability of its magnetic design. The main drawback of this kind of large, combined functions magnet, namely the interplay between the different corrections can be easily controlled due to the good linearity of the field within the good field region.

The interference of the field tails with the yoke of other magnetic components in the ring should be carefully checked during commissioning by calibrating each corrector with the beam and the closed orbit detection system.

As a consequence of all the above described measurements, the prototype has been accepted and series production authorised.

References

[1]   B. Bolli, F. Iungo, N. Ganlin, F. Losciale, M. Paris, M. Preger, C. Sanelli, F. Sardone, F. Sgamma, M. Troiani - "Measurements on SIGMA-PHI Square Corrector Prototype for the DA NE Main Rings" - DA NE Technical Note MM-14.

[2]   B. Bolli, F. Iungo, N. Ganlin, F. Losciale, M. Paris, M. Preger, C. Sanelli, F. Sardone, F. Sgamma, M. Troiani - "Measurements on SIGMA-PHI Rectangular Corrector Prototype for the DA NE Main Rings" - DA NE Technical Note MM-15.

[3]   F. Iungo, M. Modena, Q. Qiao, C. Sanelli - DA NE Magnetic Measurement Systems" - DA NE Technical Note MM-1.